# Model Reference Adaptive Position Controller with Smith Predictor for a Shaking-Table in Two Axes

Carlos Esparza, Rafael Núñez, and Fabio González

Unidades Tecnológicas de Santander – UTS, Research Group on Advanced Control – GICAV, Bucaramanga, Santander, Colombia
{carlosesfra,ing.rafaeln,fagonzarm}@gmail.com

**Abstract.** In structural behavior, the analysis of civil buildings by seismic tests has been generalized by the use of shaking tables. This method requires advanced control systems. In our research we show the implementation of a Model Reference Adaptive Control (MRAC) to control the position of a shaking table, modified by the introduction of a Smith predictor to compensate the error produced by the system delay. The mechanic is based on a Slider-crank device. The control system is implemented on a 32 bits platform by Microchip, and the control is done via a remote server using the RENATA network. The results of our adaptive control system were experimentally verified using the shaking table with a 24 kg mass as a load.

**Keywords:** Adaptive Control, MRAC, Smith Predictor, Shaking-Table, RENATA.

## 1 Introduction

Traditional control systems are sufficient to control any process in which it is knows the mathematical model of the plant, especially when the process is lineal. However, when the process model is unknown and it has non-linear components, it is necessary to implement other kind of control systems designs. These control systems should be independent from the model to control [1] [2]. One example of this problem is presented in this work, in which it is necessary to control a shaking table that is used to analyze the earthquake evaluations for tall buildings or several active antiseismic systems that decrease the oscillations of buildings subject to seismic events. Generally, shaking tables consists of electrohydraulic servo systems, hydraulic actuators, a table and sensor [3–6], but in the present work the shaking table used for the test has a different mechanism that generates the displacement on each axis table.

In this particular case, the shaking table is based on a slider-crank mechanism that uses an AC induction motor to generate the linear displacement through a mechanical system based in pulleys and with chains to articulate each axis. The motors are controlled by frequency inverters through the analog option by controlling a digital potentiometer. Figure 1 shows a blocks diagram that explains the entire system interconnection. Considering these factors, to obtain a mathematical model of the system that includes the mechanical and electrical components will be complex and with high uncertainty due to parameters that can't be measured. For that reason, a

I. Batyrshin and M. González Mendoza (Eds.): MICAI 2012, Part II, LNAI 7630, pp. 271–282, 2013.

model for each axis was obtained using identification techniques. Both models have approximations higher than 90%, and they include the delay introduced by the pulley mechanism. These models are presented in section 2.

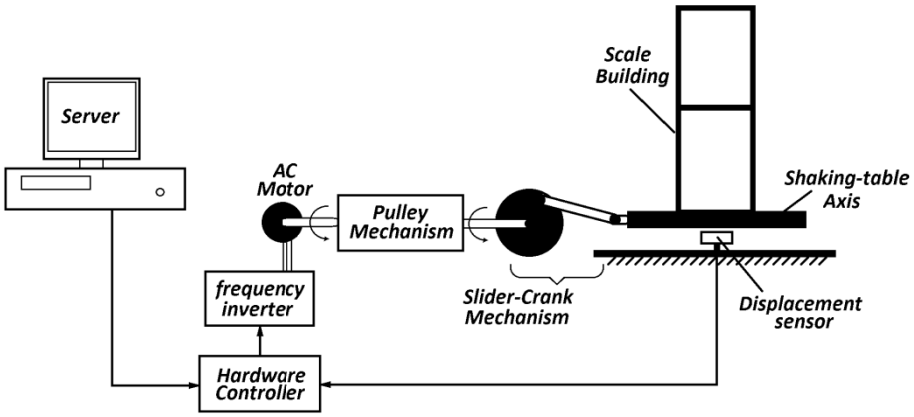


**Fig. 1.** Shaking table system interconnection

Although the implementation of an adaptive controller does not require a mathematical model to control the system, in the Model Reference Adaptive Control (MRAC) technique it is necessary to use a plant that simulates the ideal response of the system, which will be the signal that the controller try to follows to minimize the error [7]. The structure of the control system applied to our work is shown in figure 2.

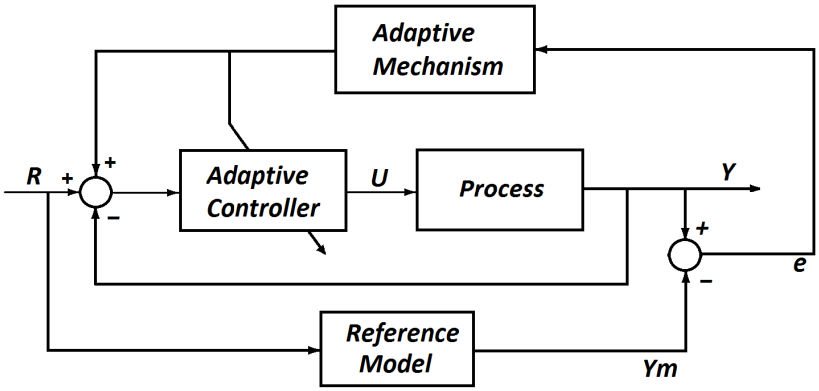


**Fig. 2.** Block diagram of MRAC Adaptive Model

A MRAC adaptive control is based on the MIT rule, so called because it was developed at Massachusetts Institute of Technology, that implements the gradient optimization technique to minimize the loss function given by equation 1, where $e$ is the signal error in figure 1 and $\theta$ the controller parameters.

$$J(\theta) = \frac{1}{2}e^2 \ . \tag{1}$$

To minimize this function, the θ parameters must change in the direction of the negative gradient of $J$ [8] [9] given by the equation 2, in which γ parameter is the adaptation gain, that must be correctly selected in order to reduce the settling time, and at the same time not rising the oscillation frequencies that cause an increase in the overshoot [10, 11].

$$\frac{d\theta}{dt} = -\gamma \frac{\partial J}{\partial \theta} = -\gamma e \frac{\partial e}{\partial \theta} = -\gamma e \left( \frac{\partial Y}{\partial \theta} - \frac{\partial Ym}{\partial \theta} \right). \tag{2}$$

The partial derivate of the error respect to the controller parameters (third term in equation 2) is the sensitivity derivative of the system. It explains how the error is affected by the adjustable controller parameters [8]. The equation 2 is the general form, and when there are several θ adjustable parameters, θ will be a vector and the partial derivate becomes in the gradient of error respect to controller parameters.

In this work, a position adaptive controller with two adaptation parameters θ ($\theta_1$ and $\theta_2$) is implemented, so that the control law is described as in equation 3 [12] [9]. Also, in this work the plant model is described by a second order plant with an integrator for the X-axis and a delay, and for simplification the delay is eliminated from the closed-loop plant model, to be added after the loop, in the same way as it is used in the Smith predictor structure. For the Y axis, the model is described in a similar way, but with a first order plant with an integrator. This is a good approximation of the model, because the changes on perturbations dynamics in the system are slow [13]. The Smith predictor structure used in this work is based in the Intern Model Control (IMC) technique as showed in figure 3.

$$U = \theta_i^T . w = \theta_1 R - \theta_2 Y \ . \tag{3}$$

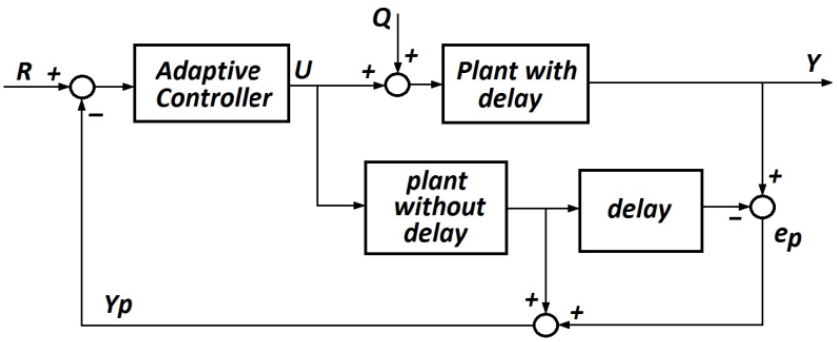


**Fig. 3.** Smith predictor control structure, IMC representation

# 2 Plant Models

## 2.1 X and Y Axes Models. Identification

The X axis (North-South component) and the Y axis (East-West component) of the shaking table are mechanical structures based on a slider-crank mechanism like it was described above, as it is shown on figure 4. To simplify the model of each axis, a linear model for displacement was obtained by the identification of a process model with transfer functions as shown in equation 4 for the X-axis and equation 5 for the Y-axis.

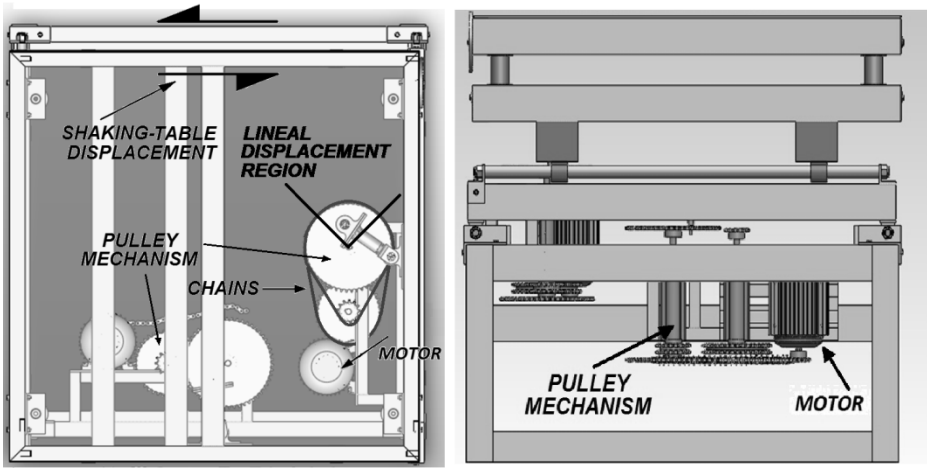


**Fig. 4.** Left: Slider-Crank mechanism used in the shaking table axis. Right: pulley mechanism.

$$G(s) = \frac{K_p . e^{-T_d * s}}{s(1 + 2.Zeta.Tw.s + (Tw.s)^2)} \ . \tag{4}$$

$$G(s) = \frac{K_p . e^{-T_d * s}}{s(1 + Tp1.s)} \ . \tag{5}$$

This lineal approximation can be made by defining the lineal displacement region of each table axis, as it is shown in figure 4, which allows a maximum displacement on each axis in the range of + 6 cm to -6 cm. In table 1 the parameters of equations 4 and 5 for X and Y axis are presented. They achieve approximations of 91.8% and 91.97% respectively. The final transfer functions are shown in equations 6 and 7, which are the plant models used for the Smith predictor in the branch without the delay.

**Table 1.** Model Parameters, obtained by identification process

| Parameters | X axis | Y axis |
|---|---|---|
| $K_P$ | 82.739 | 77.977 |
| $T_d$ | 0.075121 | 0.076994 |
| Zeta | 0.40121 | -- |
| Tw | 0.029128 | -- |
| Tp1 | -- | 0.021358 |

$$G_X(s) = \frac{82.739.e^{-0.075121s}}{s(0.0008484s^2 + 0.02337s + 1)} \ . \tag{6}$$

$$G_Y(s) = \frac{77.977.e^{-0.0077277s}}{s(0.02136\,s + \ 1)} \ . \tag{7}$$

Equations 6 and 7 are also used to obtain the reference model transfer function in the adaptive controller, and the transfer functions used in the loops that modify the control parameters θ.

### 2.2 Reference Models for X and Y Axes

From figure 2, the output of the process is the multiplication of the transfer functions of the plant $G_P(s)$ with the output of the controller $U(s)$ in Laplace domain. Given that the control output is defined by equation 3, and the plant model with delay can be approximated to a plant model without delay as it proposed in [13], the response $Y$ for X axis can be described by equation 8.

$$Y_X(s) = \frac{K_p}{s(1 + 2.Zeta.Tw.s + (Tw.s)^2)}(\theta_1 R - \theta_2 Y_X) \ . \tag{8}$$

By solving the equation 8, the closed-loop transfer function that relates the output $Y_X$ with the input $R$ of the system is:

$$\frac{Y_X(s)}{R(s)} = \frac{K_p.\theta_1}{s(1 + 2.Zeta.Tw.s + (Tw.s)^2) + K_p.\theta_2} \ . \tag{9}$$

In the same way, the closed-loop transfer function that relates the output $Y_Y$ with the input $R$ for the Y axis system is:

$$\frac{Y_Y(s)}{R(s)} = \frac{K_p.\theta_1}{s(1 + Tp1.s) + K_p.\theta_2} \ . \tag{10}$$

Equations 9 and 10 are the model-reference transfer functions used in the adaptive controllers MRAC. To complete the reference model for each axis, it is just necessary to add the delay from each plant model shown in equations 6 and 7, and given the appropriate initial values for the variable parameters $\theta_1$ and $\theta_2$ so that the reference models have the desired response for seismic signals.

## 3 Adaptive Controller Design

Once obtained the reference models, we can obtain the equations that describe the change of θ parameters by applying the adaptation MIT rule given in equation 2, but like the reference models transfer functions doesn't change with θ, the partial derivate of *Ym* respect to θ, this term can be omitted. Taken this into account, the adaptive algorithm can be obtained by:

$$\frac{\partial e}{\partial \theta} = \frac{\partial e}{\partial \theta_1} + \frac{\partial e}{\partial \theta_2} = \frac{\partial Y}{\partial \theta_1} + \frac{\partial Y}{\partial \theta_2}. \tag{11}$$

Equation 11 can be used for both axes, so the equations below are used to obtain the equations to describe the change of θ in the adaptive control.

$$\frac{\partial e}{\partial \theta_1} = \frac{\partial \left( \frac{K_p.\theta_1}{s(1+2.Zeta.Tw.s+(Tw.s)^2)+K_p.\theta_2}.R(s) \right)}{\partial \theta_1}. \tag{12}$$

$$\frac{\partial e}{\partial \theta_1} = \frac{K_p.R(s)}{s(1+2.Zeta.Tw.s+(Tw.s)^2)+K_p.\theta_2}. \tag{13}$$

$$\frac{\partial e}{\partial \theta_2} = \frac{\partial \left( \frac{K_p.\theta_1}{s(1+2.Zeta.Tw.s+(Tw.s)^2)+K_p.\theta_2}.R(s) \right)}{\partial \theta_2}. \tag{14}$$

$$\frac{\partial e}{\partial \theta_2} = \frac{-K_p.K_p.\theta_1.R(s)}{\left(s(1+2.Zeta.Tw.s+(Tw.s)^2)+K_p.\theta_2\right)^2}. \tag{15}$$

$$\frac{\partial e}{\partial \theta_2} = \frac{-K_p.Y(s)}{s(1+2.Zeta.Tw.s+(Tw.s)^2)+K_p.\theta_2}. \tag{16}$$

Based on equations 13 and 16, and by using the equation 2, the equation that describes the change of θ parameters to update the adaptive controller are:

$$\theta_1 = -\frac{\gamma.e.R(s)}{s}\left(\frac{K_p}{s(1+2.Zeta.Tw.s+(Tw.s)^2)+K_p.\theta_2}\right). \tag{17}$$

$$\theta_2 = \frac{\gamma.e.Y(s)}{s}\left(\frac{K_p}{s(1+2.Zeta.Tw.s+(Tw.s)^2)+K_p.\theta_2}\right). \tag{18}$$

It's important to notice that the reference models obtained in 9 and 10 don't include the plant delay, so the equation 17 also has to include this delay. In equation 18 it's not necessary because the term Y(s) already includes the delay since it corresponds to the real output plant. Also, in equations 17 and 18 and in the reference models equations 9 and 10 as well, all the parameters are fixed, and they correspond to the initial parameters values obtained by a tuning process of the system. These values are shown in table 2.

**Table 2.** Initial Adaptive Control Parameters

| Parameters | X axis | Y axis |
|---|---|---|
| $\gamma$ | 0.0003 | 0.00035 |
| $\theta_1$ | 0.08 | 0.05 |
| $\theta_2$ | 0.08 | 0.05 |

Figure 5 shows the blocks diagram of the adaptive controller with Smith predictor used for both axes. Equations 19 to 22 are the final transfer functions for X axis and equations 23 to 26 the transfer functions for Y axis controllers.

$$Reference\_Model_X = \frac{6.619.e^{-0.0751s}}{0.0008484\,s^3 + 0.02337\,s^2 + s + 6.619} \quad . \tag{19}$$

$$Plant\_without\_delay_X = \frac{82.74}{0.0008484\,s^3 + 0.02337\,s^2 + s} \quad . \tag{20}$$

$$Model_X\_\theta_1 = \frac{82.74.e^{-0.0751s}}{0.0008484\,s^3 + 0.02337\,s^2 + s + 6.619} \quad . \tag{21}$$

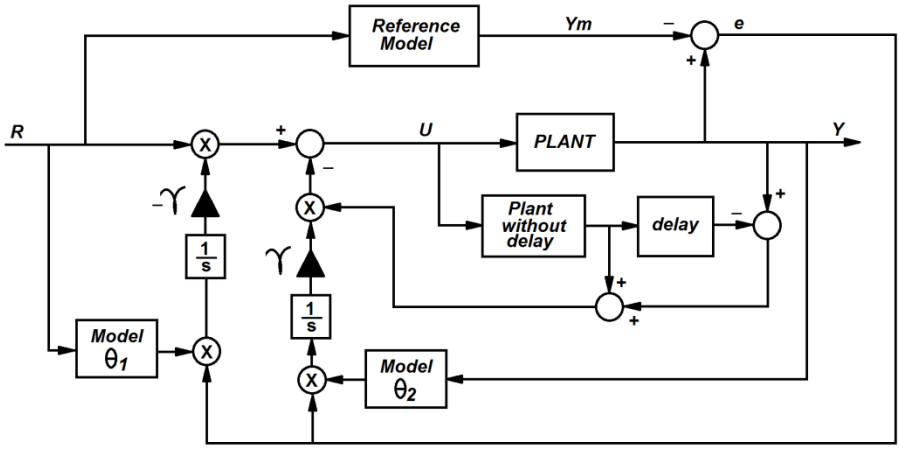


**Fig. 5.** Blocks Diagram of the Adaptive Control Implemented in X and Y axes

$$Model_X\_\theta_2 = \frac{82.74}{0.0008484\,s^3 + 0.02337\,s^2 + s + 6.619} \quad . \tag{22}$$

$$Reference\_Model_Y = \frac{3.899.e^{-0.077s}}{0.02136\,s^2 + s + 3.899} \quad . \tag{23}$$

$$Plant\_without\_delay_Y = \frac{77.98}{0.02136\,s^2 + s} \quad . \tag{24}$$

$$Model_Y\_\theta_1 = \frac{77.98.e^{-0.077s}}{0.02136\,s^2 + s + 3.899} \quad . \tag{25}$$

$$Model_Y\_\theta_2 = \frac{77.98}{0.02136\,s^2 + s + 3.899} \quad . \tag{26}$$

## 4 Results

Once the controllers for X and Y axis were tuned using a simulation process, they were implemented on a 32 bits microcontroller platform by Microchip. This hardware is connected to a sever via serial connection through two XBee devices. The sample frequency used is 200 Hz, which is enough for the shaking table system used to generate the seismic signals, whose higher frequency components are up to 30 Hz. All the transfer functions were converted to difference equations in Z domain using a zero order hold and they were programmed in the hardware device.

Figure 6 shows the results for the test of the adaptive controllers implemented on the hardware device when the input signal is a periodic stair sequence. According to the figure, we can see the faster response adaptation of the system that follows the reference model in the second transient of the input signal.

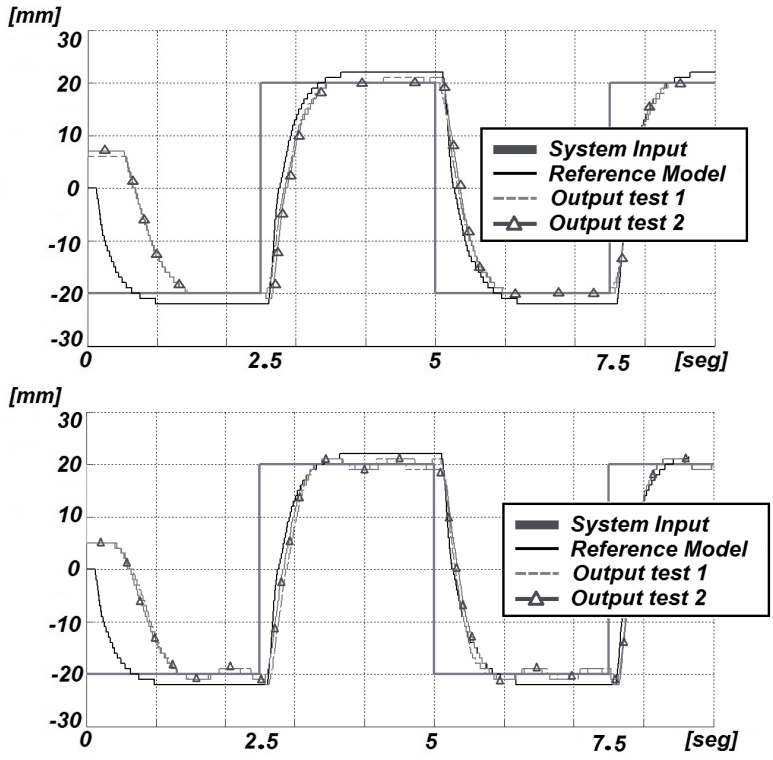


**Fig. 6.** Results for the Adaptive Controllers implemented on the hardware device. up) X-axis, down) Y-Axis.

The results presented in figure 6 shows that the adaptive controller response has high level approximation and repeatability for the different tests made on the shaking table. In this case, to analyze the approximation between the desired signal given by the reference model and the obtained signal we can use a measurement Normalized Root Mean Square Error – NRMSE, given in equation 27 [14], and the measurement of the amount of variability between the signals using the coefficient of determination $R^2$ described in equation 28 [15]. In both cases, the NRMSE and the $R^2$, two values are obtained, one for all the samples in the test and the other eliminating the first samples that takes the system to follow the reference model, that is approximately 2,5 seconds.

$$NRMSE = \sqrt{\frac{\sum_{i=1}^{n}(x_i - y_i')^2}{\sum_{i=1}^{n}(x_i)^2}} \quad . \tag{27}$$

$$R^2 = 1 - \frac{\sum_{i=1}^{n}(x_i - y_i')^2}{\sum_{i=1}^{n}(x_i - \mu_{xi})^2} = 1 - \frac{var(e)}{var(x_i)} \quad . \tag{28}$$

Table 3 shows the results obtained in 4 tests made on the shaking table with the periodic stair sequence for the X-axis, and Table 4 shows the same results for the Y-axis.

**Table 3.** NRMSE and $R^2$ results for X-axis

| Test | All samples | | Without first 2.5 seconds | |
|---|---|---|---|---|
| | NRMSE | $R^2$ | NRMSE | $R^2$ |
| 1 | 0.20405 | 95.936 | 0.12073 | 98.536 |
| 2 | 0.20539 | 95.919 | 0.11419 | 98.689 |
| 3 | 0.21033 | 95.703 | 0.12475 | 98.435 |
| 4 | 0.21929 | 95.411 | 0.13463 | 98.191 |

**Table 4.** NRMSE and $R^2$ results for Y-axis

| Test | All samples | | Without first 2.5 seconds | |
|---|---|---|---|---|
| | NRMSE | $R^2$ | NRMSE | $R^2$ |
| 1 | 0.19373 | 96.272 | 0.12689 | 98.412 |
| 2 | 0.18681 | 96.547 | 0.12339 | 98.484 |
| 3 | 0.19321 | 96.322 | 0.1298 | 98.313 |
| 4 | 0.2023 | 95.968 | 0.13867 | 98.073 |

Finally, figure 7 shows the results when the input of the system is a seismic signal, that for the test is the data collected from Imperial Valley, CA earthquake of October 15 1979. This earthquake was selected because has low frequency components, ideal for experiments in this shaking table, and was downloaded from the Center of Engineering Strong Motion Data (CESMD). However, in these results can be noticed that the Y-axis seismic tests have a slower adaptation time than for the X-axis. This is because the initial transitions of displacement in Y-axis have small values, lower than 10 millimeters unlike the X-axis.

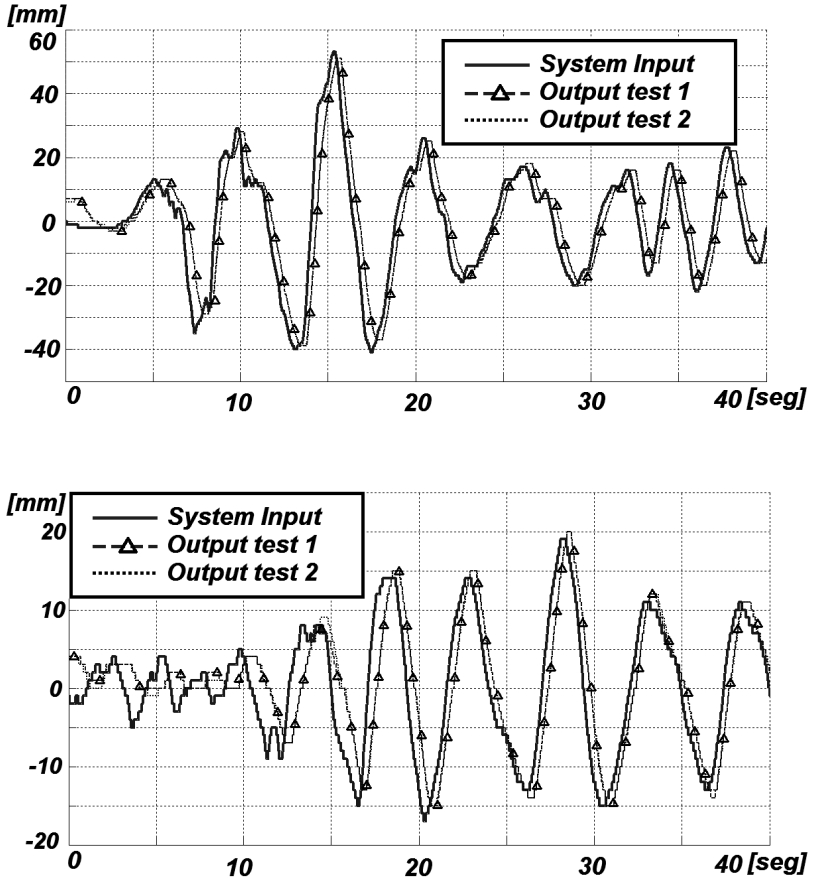


**Fig. 7.** Results for the Adaptive Controllers for seismic displacement signals. up) X-axis, down) Y-Axis

## 5 Conclusions

The results of this work show that the control system of a plant with high uncertainty and with delay can be done by implementing a reference model adaptive controller, for which it is only necessary to have a general knowledge of the dynamic behavior of the plant. In consequence, it was possible to implement an adaptive control algorithm with two adaptation parameters based on the rule MIT, modifying their structure to introduce a Smith predictor model which improves the performance of the controller by compensating the error generated in the difference equation due to the system delay.

Also, it was verified that the system delay can be handled outside of the closed-loop, so that the reference model can be easier to manipulate, obtaining an approximate response to those of the real system.

Moreover, although it wasn't mentioned in the document, the sensor resolution used for feedback is 1 millimeter, given by an encoder with 100 pulses per revolution. The response of the system is appropriate despite the error that is introduced by the rounding, obtaining ratios between the desired signals and the output signals above 90%. For this reason, the sensors will be improved for further works with the shaking table system.

On the other hand, the problem of the slow time for the adaptation in the Y-axis that appears for the amplitude of the input signal can be improved with the normalization of the MIT rule like is proposed by Astrom in [8], so that no matter what is the value of the input signal or the value for the adaptation gain value, the adaptive controller will always follow the reference model at the same speed.

Finally, the first test for the remote access to the system works properly over a LAN network, and currently it is validating over the RENATA network, through which it is intended to launch a digital control system laboratory based on the shaking table system.

## References

1. Landau, I.D., Lozano, R., M'Saad, M., Karimi, A.: Adaptive Control: Algorithms, Analysis and Applications, 2nd edn. Springer (2011)
2. Tu, J.W., Jiang, S.J., Stoten, D.P.: The Seismic Response Reduction by Using Model Reference Adaptive Control Algorithm. In: 2010 International Conference on Mechanic Automation and Control Engineering (MACE), pp. 1215–1218. IEEE (2010)
3. Chen, J., Zhang, X., Tan, P., Wei, L.: Analysis of the Electro-hydraulic Servo Shaking Table with Flexible Payload. Technology, 708–713 (2009)
4. Seki, K., Iwasaki, M., Kawafuku, M., Hirai, H., Yasuda, K.: Adaptive Compensation for Reaction Force With Frequency Variation in Shaking Table Systems. IEEE Transactions on Industrial Electronics 56, 3864–3871 (2009)
5. Gavin, H.P., Hoagg, J.B.: Control Objectives for Seismic Simulators. Control, 3932–3937 (2009)
6. Seki, K., Iwasaki, M., Hirai, H.: Reaction Force Compensation With Frequency Identifier in Shaking Table Systems. Control, 673–678 (2010)
7. Rodríguez Rubio, F., López Sánchez, M.J.: Control Adaptativo y Robusto. Secretariado de Publicaciones de la Universidad de Sevilla (1996).
8. Astrom, K.J., Wittenmark, B.: Adaptive Control, 2nd edn. Addison-Wesley Longman Publishing Co. Inc. (1994)
9. Duraisamy, R., Dakshinamurthy, S.: An adaptive optimisation scheme for controlling air flow process with satisfactory transient performance. Maejo International Journal of Science and Technology 4, 221–234 (2010)
10. Swarnkar, P., Jain, S., Nema, R.K.: Effect of adaptation gain in model reference adaptive controlled second order system. Engineering, Technology & Applied 1, 70–75 (2011)

11. Stellet, J.E.: Influence of Adaptation Gain and Reference Model Parameters on System Performance for Model Reference Adaptive Control. World Academy of Science, Engineering and Technology 60, 1768–1773 (2011)
12. Ioacnou, P.: Chapter 54. Model Reference Adaptive Control. In: The Control Handbook, pp. 847–858. CRC Press, IEEE Press (2000)
13. Normey-Rico, J.E., Camacho, E.F.: Predicción Para Control: Una Panorámica del Control de Procesos con Retardo. Revista Iberoamericana de Automática e Informática Industrial - RIAI 3, 5–25 (2006)
14. Frýza, T., Hanus, S.: Video signals transparency in consequence of 3D-DCT transform. In: Radioelektronika 2003 Conference Proceedings, pp. 127–130 (2003)
15. Montgomery, D.C., Runger, G.C.: Applied Statistics and Probability for Engineers, 3rd edn. John Wiley & Sons, Ltd. (2003)